

## EXTENDED-RANGE GLUCOSE BIOSENSOR VIA LAYER-BY-LAYER ASSEMBLY INCORPORATING GOLD NANOPARTICLES

Wei Zhao, Jing-Juan Xu\* and Hong-Yuan Chen

Key Lab of Analytical Chemistry for Life Science, Department of Chemistry, Nanjing University, Nanjing 210093, P.R. China

### TABLE OF CONTENTS

1. Abstract
2. Introduction
3. Experimental
  - 3.1. Regents
  - 3.2. Preparation of gold nanoparticles
  - 3.3. Preparation of the PDDA/PSS/(PDDA/Au<sub>NP</sub>/PDDA/GOx)<sub>n</sub> multilayer films
  - 3.4. Electrochemical Measurements
  - 3.5. UV-Visible Absorption Spectroscopic Measurements.
4. Result and discussions
  - 4.1. Formation of multilayer structure
  - 4.2. Electrochemical Impedance Characterization of PDDA/Au<sub>NP</sub>/PDDA/GOx Multilayers
  - 4.3. UV-Visible Absorption Spectroscopy Characterization of PDDA/Au<sub>NP</sub>/PDDA/GOx Multilayers
  - 4.4. Multilayer Films as Sensing Elements for Glucose Detection
  - 4.5. Optimal Number of Multilayers for glucose response
  - 4.6. Effect of the Solution pH on the Biosensor Response
  - 4.7. The Reproducibility and Stability of Biosensor
5. Conclusion
6. Acknowledgement
7. References

### 1. ABSTRACT

We report on a glucose oxidase (GOx)/polyelectrolyte (PE)/gold nanoparticle (AuNP) multilayer films that can be utilized as efficient glucose biosensors by layer-by-layer self-assembly method. Electrochemical impedance spectroscopy (EIS) and UV-visible spectroscopy were adopted to monitor the regular growth of the multilayer films. The role of gold nanoparticles integrated in the multilayer films not only increase the amount and activity of GOx, but also significantly improve the electron-transfer characteristics of the films. The performance of the multilayer films for sensing glucose could be tailored by controlling the gold nanoparticles loading in the film and the number of layers. A biosensor constructed by four poly(dimethyldiallylammonium chloride) (PDDA)/Au<sub>NP</sub>/PDDA/GOx multilayer films exhibited a wide linear calibration range from 0 to 60.0 mM with the detection limit of 3.0  $\mu$ M for the detection of glucose. The dynamic range can be extended up to 120 mM. The biosensor has good stability and reproducibility.

### 2. INTRODUCTION

Considerable efforts have been devoted to the design of amperometric enzyme biosensors for the clinical, environmental, and food analysis during the past decade [1-8]. With regard to enzyme sensors, linear range and sensitivity are two of the most important factors discussed in published papers [9-21]. Several routes have been proposed for enhancing the sensitivity [9, 10]. For glucose biosensors, generally, the factors that result in high sensitivity not always result in suitable linear range.

Smaller Michaelis constant of an immobilized enzyme for a substrate is, higher the sensitivity of the biosensor is [11]. The Michaelis constant of an immobilized enzyme is largely influenced by immobilization approach and matrix. It was reported that enzymes adsorbed on nanoparticles such as gold nanoparticles could retain their bioactivity [22, 23], due to the large specific surface area and increased biocompatibility of nanoparticles. For example, Chen et al. [24] constructed a glucose biosensor based on chitosan-glucose oxidase-gold nanoparticles biocomposite formed by one-step electrodeposition. The decorated gold nanoparticles in the biocomposite offers excellent affinity to enzyme with a detection limit of 2.7  $\mu$ M. However the upper limit of the linear range only up to 2.4 mM. In order to extend the dynamic range, various approaches were attempted [12-21]. Increasing the oxygen/glucose permeability ratio is one approach to extend the dynamic range of glucose oxidase-based biosensor [12-15]. One commonly used strategy relies on the use of mass-transport limiting films for tailoring the flux of glucose and oxygen. However, this method usually suffers from low sensitivity [14, 15]. The second approach to extend the dynamic range of a biosensor is using a fast redox mediator instead of oxygen, such as ferrocene [16-20]. The mediator can enhance the electron transfer cycle and consequently increases the numbers of the GOx catalytic reaction at a certain period when the concentration of glucose is around  $k_{mapp}$ . This method not only offers a somewhat large dynamic range for the detection of glucose, but also decreases the working electrode potential. However the immobilization of mediator will result in other problems such as less stability [19] or complicated procedures [20].

The third method is using composite-engineered enzymes with different Michaelis constants. For example, Koji Sode and his colleagues reported an extended-range glucose sensor employing composite engineered glucose dehydrogenases with different Michaelis constants [21]. The dynamic range was extended up to 70 mM. It was a good idea for preparing sensitive glucose biosensor with extended dynamic range, except that the preparation procedure of engineered enzymes was somewhat complicated and an electron mediator (such as phenazine methosulfate) should be present in solution. Therefore, how to use simple method to fabricate glucose biosensors with both extended linear range and high sensitivity is still a challenge for the researchers.

The layer-by-layer (LBL) assembly method developed by Decher in 1991 was proved to be possible to build-up ordered multilayer structures by consecutive adsorption of polyanions and polycations [25]. In 1995 this new method was applied to immobilize negatively charged GOx in a polyethyleneimine based multilayer structure [26] and proved to be one of the most perspective methods for preparing amperometric enzyme biosensors. One year later, an oxygen mediated glucose biosensor based on GOx and poly(L-lysine) coadsorbed onto a negatively charged monolayer of mercaptopropionic acid, deposited on an Au electrode was described [27]. In 1997, Chen et al. [28] and Hodak et al. [29] simultaneously reported a reagentless glucose biosensor based on this technique by the successive alternate deposition of ferrocene attached polypyridine or ferrocene modified poly(allylamine) (cationic) polymer and anionic GOx, on Au electrode surface, initially thiolated with negatively charged sulfonic groups. Since then, this method have been widely used to fabricate glucose biosensors via integrating various mediators such as complex osmium redox polymer [30-35], ferrocenyl-tethered dendrimers (Fc-D) [36], 1,4-diaminoanthraquinone (DAAQ) [37] into the multilayer films for the construction of glucose biosensors, or combining GOx with other enzymes such as lactate oxidase (LOx), ascorbate oxidase (AOx) and horseradish peroxidase (HRP) to develop bienzyme multilayer films for the preparation of biosensors [31, 38-40]. These glucose biosensors have several advantages: the thickness of the enzyme film can be regulated precisely at molecular level and the geometry of multi-enzyme thin films is optimized easily by changing the sequence of deposition [39,41]. In addition, the response of the multilayer-modified sensors increases and the linear range extends with increasing number of the enzyme layers [36,42]. Nevertheless, the largest upper limit of the linear concentration range of these biosensors is 20mM for single enzyme system and 30mM for bienzyme system. Recently, the LBL technology also has been successfully applied to the preparation of thin films of nanoparticles such as metal nanoparticles [43,44] and various other inorganic materials[45,46]. The resulted assembly exhibits specific characteristics in the multilayer films, and the optical and electronic properties of the films can be changed by integrating various nanoparticles with different characteristics [43-48]. Gold nanoparticles have excellent catalytic activity due to their high surface area-to-volume ratio and their interface-dominated properties are

significantly different from their bulk counterparts [49,50]. Recently efforts have been devoted to the integration of gold nanoparticles into multilayer films for various applications such as sensors and nanodevices [47,51-54]. Frank Caruso and co-workers reported an electrochemical sensor prepared by infiltrating DMAP-gold nanoparticles into polyelectrolyte multilayer films preassembled on ITO electrodes and showed that the electron transfer characteristics of the films improved significantly [51]. Tobias Vossmeier and co-workers investigated the optical and electrical properties of layer-by-layer self-assembly of gold nanoparticle/alkanedithiol films [54]. Though gold nanoparticles or enzymes have been widely used to form multilayer films by layer-by-layer technology, the strategy of integrating both gold nanoparticles and enzymes into one polyelectrolyte multilayer film via layer-by-layer assembly to construct biosensors has not been reported previously, to our knowledge.

In this paper, we immobilized gold nanoparticles ( $Au_{NP}$ ) and glucose oxidase in PDDA films by layer-by-layer self-assembly to construct  $(PDDA/Au_{NP}/PDDA/GOx)_n$  multilayer films for developing glucose biosensors. The novel multilayer films were characterized by UV-visible absorption spectroscopy and the electrochemical impedance spectroscopy (EIS). With the introduction of gold nanoparticles, not only the amount and the activity of GOx, but also the electron transfer characteristics of the films improved. As a result, the performance of the biosensor was improved. A wide dynamic range (up to 120mM) and a low detection limit (down to 3.0  $\mu$ M) were obtained in four  $PDDA/Au_{NP}/PDDA/enzyme$  multilayer films.

### 3. Experimental

#### 3.1. Reagents

GOx (E. C. 1.1.3.4, type X-S, 179 units  $mg^{-1}$ ) were purchased from Sigma.  $HAuCl_4 \cdot 4H_2O$  ( $Au\% > 48\%$ ), poly(dimethyldiallylammonium chloride) (PDDA)  $M_w = 100,000-200,000 g mol^{-1}$  in 20% aqueous solution, poly(sodium 4-styrenesulfonate) (PSS)  $M_w = 70,000 g mol^{-1}$  in 30% aqueous solution, 3-mercapto-1-propanesulfonic acid, sodium salt (MPS) and Nafion (product no. 27470-4) were purchased from Aldrich. All other chemicals were of analytical grade and were used as received. Twice-distilled water was used throughout.

#### 3.2. Preparation of gold nanoparticles

All glasswares used in the following procedures were cleaned in a bath of freshly prepared 3:1  $HNO_3-HCl$  solution, thoroughly rinsed with water and dried in air.  $HAuCl_4$  and trisodium citrate solutions need to be filtered through a 0.22  $\mu m$  microporous membrane filter prior to use. Preparations were stored in brown glass bottles at 4°C. Gold nanoparticles were prepared according to the literature [55] with a little modification. Briefly, 2.50 mL of 1% trisodium citrate was added to 100 mL of boiling 0.01%  $HAuCl_4$  solution. The particle sizes were about 17 nm, which were measured by transmission electron microscopy (TEM). The concentration of gold nanoparticles was about 1.6 nM, which was calculated according to the amount of starting material, the density of

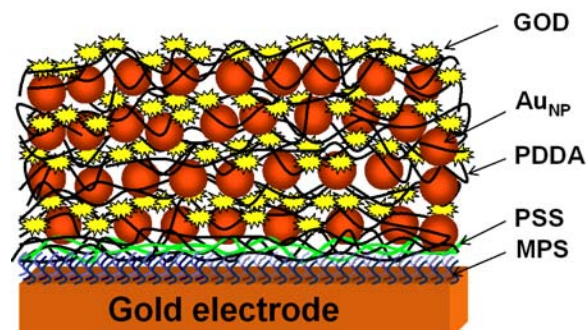


Figure. 1 Idealized structure of multilayer films

gold, the approximate size of the nanoparticles and assuming the reaction yield of 100% [56]. The solution was diluted as needed for the experiments.

### 3.3. Preparation of the PDDA/PSS/(PDDA/AuNP/PDDA/GOx)<sub>n</sub> multilayer films

Bulk gold disk electrodes were abraded with fine SiC paper and polished carefully with 0.3 and 0.05 μm alumina slurry, and sonicated in water and absolute ethanol. The negatively charged surface (Au/MPS) was prepared by immersing the cleaned gold electrode into a 2 mM MPS aqueous solution for 8h, and then washed with distilled water.

The procedure for preparing PDDA/PSS/(PDDA/AuNP/PDDA/GOx)<sub>n</sub> multilayer films was as follows. For substrate modification, gold electrodes with negatively charged surface were respectively treated by a PDDA aqueous solution (2mg/ml) and a PSS aqueous solution (2mg/ml) for 15 min before LBL assembly. After the treated substrates were washed with distilled water, multilayer films were grown by alternate dipping of the modified gold electrodes into the positively charged PDDA aqueous solution (2mg/ml), the negatively charged gold nanoparticles, the positively charged PDDA aqueous solution (2mg/ml) and the negatively charged GOx (pH=7.4) for 15 min, respectively. The films were carefully washed with distilled water after each dipping step. This sequence was repeated to obtain the desired number of layers. For comparison, the multilayer films without gold nanoparticles were prepared alike, thus PDDA/PSS/(PDDA/GOx)<sub>n</sub> modified gold electrodes were obtained.

Glass slides (0.8×4 cm<sup>2</sup>, 1 mm thick) were washed in a washing solution (49% ethanol: 50% water: 1% KOH) for 30 min at 50 °C, and rinsed with water to introduce negative charges on the glass surface. Layer-by-layer films of PDDA/PSS/(PDDA/AuNP/PDDA/GOx)<sub>n</sub> were then assembled on the glass slides in the same way as on the MPS modified Au electrodes as described above.

### 3.4. Electrochemical Measurements

Amperometric experiments were performed on a CHI 750A electrochemical workstation (Shanghai Chenhua Apparatus corporation, China). All experiments were carried out using a conventional three-electrode system with the gold disk electrode as the working electrode, a platinum foil as the auxiliary electrode, and a saturated

calomel electrode as the reference one. In steady-state amperometric experiments, the potential was set at 700 mV with a magnetic stirring. Electrolyte solutions were deoxygenated by bubbling with high-purity nitrogen prior to and blanketed with nitrogen during electrochemical experiments.

The electrochemical impedance spectroscopy (EIS) measurements were also conducted by the CHI 750A electrochemical workstation with a three-electrode system in the presence of 5.0×10<sup>-3</sup> mol/L K<sub>3</sub>[Fe(CN)<sub>6</sub>]/K<sub>4</sub>[Fe(CN)<sub>6</sub>], 1:1 mixture, as a redox probe. The amplitude of the applied sine wave potential was 5 mV at the bias potential equal to the redox probe's formal potential, 0.18V. The EIS was recorded with the frequency range of 0.05 Hz to 10 kHz in the form of complex plane diagrams (Nyquist plots).

### 3.5. UV-Visible Absorption Spectroscopic Measurements

Ultraviolet and visible (UV-Vis) absorption spectra were recorded with a Lambda 35 UV/VIS spectrometer (Perkin-Elmer instruments, USA). Absorbance intensities of gold nanoparticles and GOx assembly on glass substrates with increasing number of multilayer films from 1 to 8 were investigated.

## 4. RESULT AND DISCUSSION

### 4.1. Formation of multilayer structure

In pH 7.4 phosphate buffer, glucose oxidase is negatively charged. This negative charge on the surface of the enzyme makes it suitably incorporated in polyelectrolyte(PE) multilayer films, beginning with a positively charged PE. Initially, a base layer of MPS is deposited onto a gold electrode surfaces via self-assembly. The resulting hydrophilic and negatively charged surface promotes the electrostatically driven deposition of positively charged PDDA. In order to obtain a uniform and smooth charged surface for stable adsorption of enzyme layers, the substrates were further immersed in PSS and PDDA solutions alternatively, and form a PDDA/PSS/PDDA “precursor” film. With the surface sufficiently overlaid with positive charges, the enzyme molecule or gold nanoparticles can be deposited by immersing the substrates into an enzyme solution or gold colloid solution. Sequential repetition of the steps, that is, deposition of PDDA, nanoparticles and enzyme, for up to 8 times led to the systematic stacking of PDDA/AuNP/PDDA/GOx sandwich layers. Figure 1 shows the structure of multilayer films. Evidence for the uniform packing is obtained from electrochemical impedance data and absorption spectra taken after each sandwich layers increment below.

### 4.2. Electrochemical Impedance Characterization of PDDA/AuNP/PDDA/GOx Multilayers.

A Nyquist diagram of the electrochemical impedance spectrum is an effective way to measure the electron-transfer resistance. Figure 2A shows the results of impedance spectroscopy on modified electrodes with various (PDDA/AuNP/PDDA/GOx)<sub>n</sub> layer numbers (1-8) in

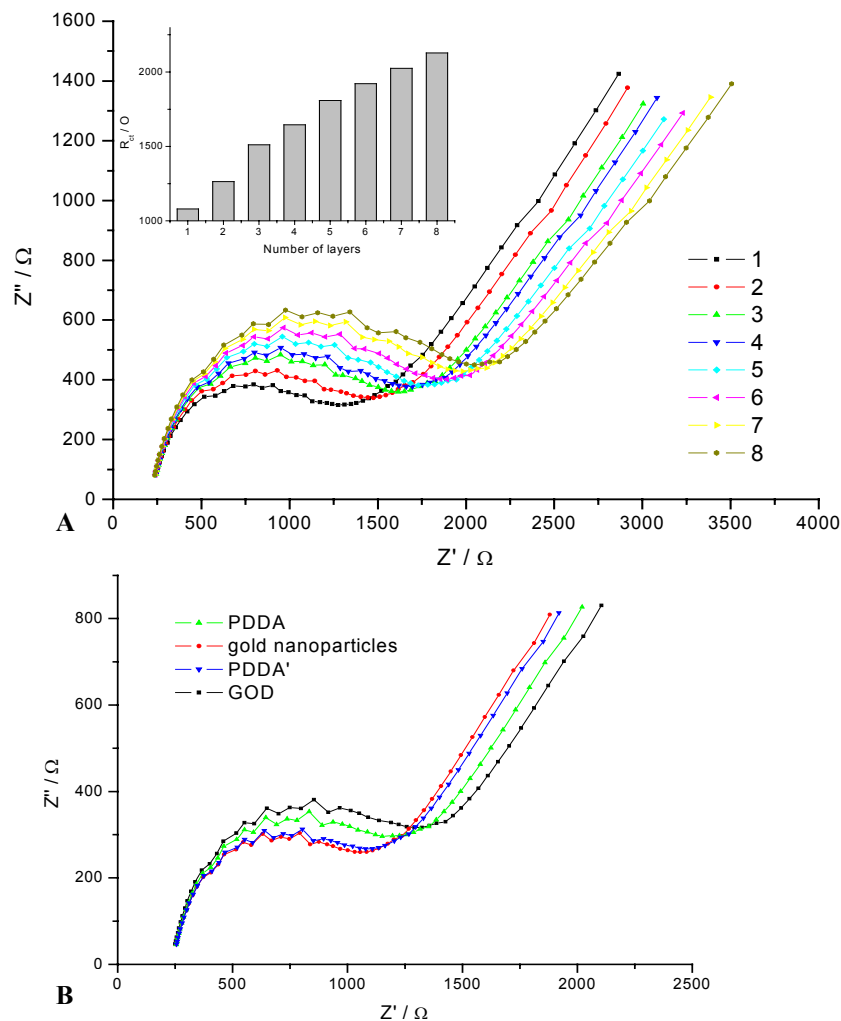


**Figure 2.** **A** Nyquist plots of the electrochemical impedance spectroscopy (EIS) of the gold electrode with (PDDA/Au<sub>NP</sub>/PDDA/GOD)<sub>n</sub> multilayer films with n=1, 2, ..., 8. Shown in the insert is a plot of the  $R_{et}$  vs. the number of PDDA/Au<sub>NP</sub>/PDDA/GOD layer. **B** Nyquist plots of EIS of the gold electrode with layers of PDDA, gold nanoparticles, PDDA' and GOD in the first PDDA/Au<sub>NP</sub>/PDDA/GOD layer.

the presence of equimolar 2.5 mM  $[\text{Fe}(\text{CN})_6]^{4-/3-}$  + 10 mM PBS + 0.1 M KCl, which are measured at the formal potential of  $[\text{Fe}(\text{CN})_6]^{4-/3-}$ . As shown in Figure 2A, each of the impedance spectra includes a semicircle portion and a linear line portion, which correspond to the electron transfer process and diffusion process, respectively. The diameter of the semicircle represents the electron-transfer resistance at the electrode surface. For a bare gold electrode, the impedance spectra exhibit an almost straight line (data not shown) that is just the characteristic of the diffusional limiting step of the electrochemical process. Whereas, after the adsorption of PDDA/Au<sub>NP</sub>/PDDA/GOx multilayer, we can observe clearly from Figure 2A that the diameters of the semicircle parts increased gradually with the layer numbers increased. This increasing of the diameters indicates that the charge-transfer rate of

$[\text{Fe}(\text{CN})_6]^{4-/3-}$  becomes reduced gradually. It is attributed to the hindrance effect to the redox couples, which is caused by the deposition of PDDA/Au<sub>NP</sub>/PDDA/GOx multilayers on electrode surface. Upon the stepwise multilayer formation, it becomes more and more difficult for  $[\text{Fe}(\text{CN})_6]^{4-/3-}$  to access the electrode surface to react. The respective semicircle diameters correspond to the interfacial electron-transfer resistance  $R_{et}$ . Here,  $R_{et}$  reflects the electron-transfer kinetics of  $[\text{Fe}(\text{CN})_6]^{4-/3-}$  at the electrode interface. The value of  $R_{et}$  depends on the dielectric and insulating features at the electrode/electrolyte interface. Because enzyme and PDDA are both nonconductive, their multilayer films will block the electron-transfer of  $[\text{Fe}(\text{CN})_6]^{4-/3-}$  and  $R_{et}$  should increase gradually. The insert of Figure 2A shows a good linear relationship between  $R_{et}$  and layer numbers, indicating a well behaved LBL assembly process.

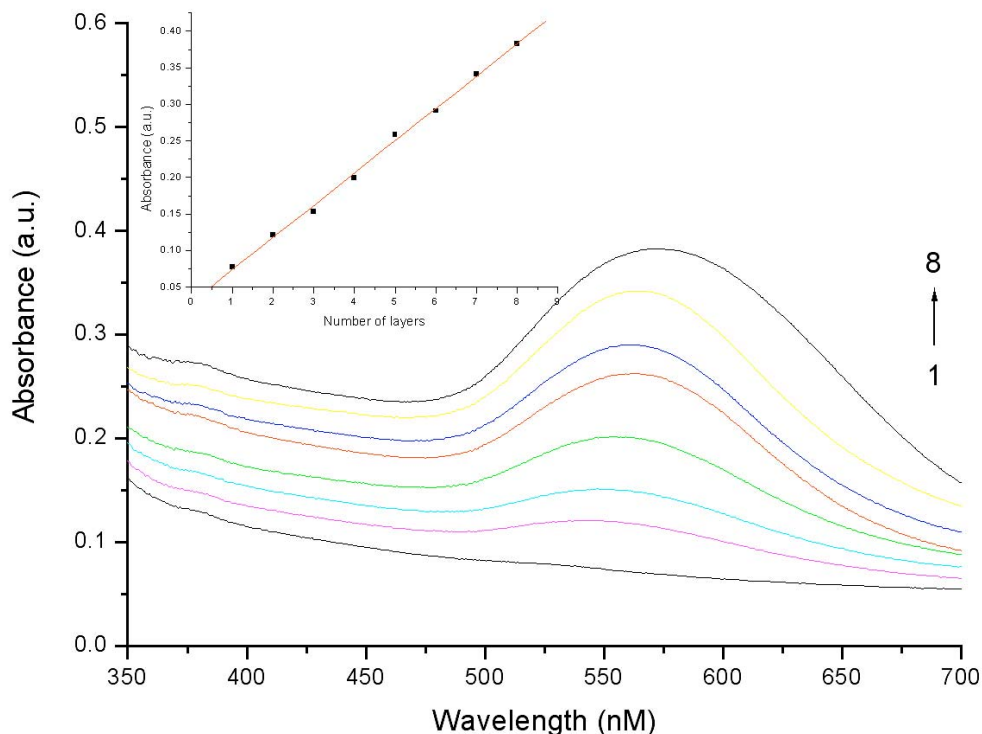


**Figure. 3** UV-visible absorption spectra of (PDDA/Au<sub>NP</sub>/PDDA/GOD)<sub>n</sub> multilayer films with different numbers. From the lower to upper curves, the number of PDDA/Au<sub>NP</sub>/PDDA/GOD layer is 1, 2, 3, 4, 5, 6, 7 and 8. Shown in the insert is a plot of the absorbance at 560 nm vs. the number of PDDA/Au<sub>NP</sub>/PDDA/GOD layer.

Furthermore, gold nanoparticles in the polyelectrolyte multilayer films could significantly improve the electron-transfer characteristics of the films. Figure 2B exhibits curves of the impedance spectroscopy of gold electrodes with the successive deposition of PDDA, gold nanoparticles, PDDA, GOx to form the first layer of PDDA/AuNP/PDDA/GOx film. As we can see, with the introduction of gold nanoparticles, the  $R_{ct}$  decreases apparently. This reveals that the gold nanoparticles in the multilayer films, acting as “electron antennae”, effectively contribute electron transfer throughout the films and improve the electron transfer between  $Fe(CN)_6^{3-/4-}$  and the electrode.

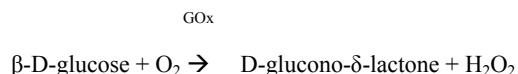
#### 4.3 UV-Visible Absorption Spectroscopy Characterization of PDDA/AuNP/PDDA/GOx Multilayers

Gold nanoparticles and GOx have their characteristic absorptions in the UV-vis region, and UV-vis spectroscopy was employed to follow the deposition process of the multilayer films. The films were prepared by alternate deposition of positively charged PDDA, negatively charged gold nanoparticles, PDDA and negatively charged GOx on a glass slide by the LBL method. Assuming that the absorption intensity is proportional to the concentration of the gold nanoparticles and GOx, the buildup of the multilayer films can be estimated from UV-vis absorption spectroscopy. Figure 3 shows the UV-visible spectroscopy of the multilayer films with different number of layers and GOx existing in the

outermost layer. It is clear that the multilayer adsorption of the PDDA/AuNP/PDDA/GOx assemblies is reproducible with sequential deposition. The strong band (560 nm) is due to the plasmon absorption of gold nanoparticles. It increases linearly with the number of deposited PDDA/AuNP/PDDA/GOx layers with a correlation coefficient of 0.998 (Figure 3, insert), suggesting that gold nanoparticles can form layer-by-layer films with GOx, and the amounts of gold nanoparticles adsorbed in each multilayer was almost the same. Thus, it is possible to precisely control the amount of material deposited simply by controlling the number of dippings. The linear increase of the intensity of the absorption band as a function of the number of successive coating is consistent with a well-behaved LBL assembly process as described previously [57,58].

#### 4.4 Multilayer Films as Sensing Elements for Glucose Detection

The sensor response is due to the following enzymatic reaction:



The hydrogen peroxide generated in this reaction can be electrochemically oxidized at a gold disk electrode. The electrode is polarized at +700 mV compared to the saturated calomel electrode.

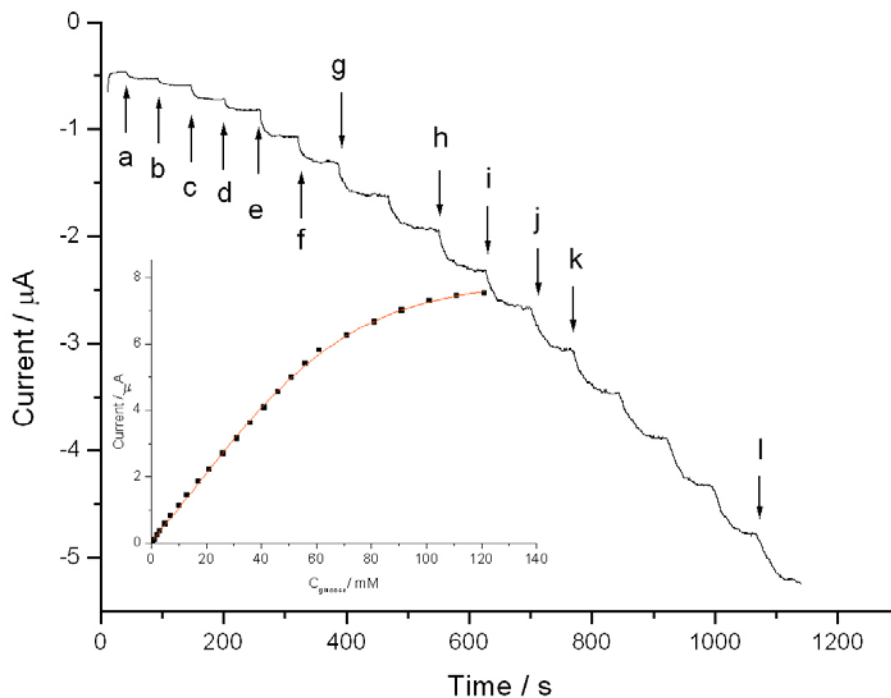


**Figure. 4** Typical amperometric response of the biosensor for glucose in a stirring phosphate buffer (pH 7.4) by successive injection of glucose with a→b, 0.5mM, c→d, 1mM, e→f, 2mM, g→h, 3mM, i→j, 4mM, k→l, 5mM. The applied potential was 0.7 V. Inset: the calibration curve of the (PDDA/Au<sub>NP</sub>/PDDA/GOD)<sub>4</sub> modified biosensor.



The typical steady-state amperometric response of (PDDA/Au<sub>NP</sub>/PDDA/GOX)<sub>4</sub> modified electrodes on successive addition of glucose is shown in Figure 4. A subsequent addition of glucose to the stirring PBS provokes a remarkable increase in the oxidation current, and the time required to reach the 95% steady state response is within  $42 \pm 2$  s. The insert of Figure 4 shows the corresponding calibration curve. The dynamic range is extended up to 120 mM, and the linear calibration range is 0 – 60.0 mM ( $r = 0.999$ ,  $n = 14$ ) with the detection limit of 3.0  $\mu\text{M}$ . The wide linear calibration range makes the biosensor suitable for the detection of glucose with high concentration.

For comparison, we prepared (PDDA/GOX)<sub>n</sub> multilayer films. Both the linear calibration range and response current of the (PDDA/Au<sub>NP</sub>/PDDA/GOX)<sub>n</sub> modified biosensor are obviously larger than (PDDA/GOX)<sub>n</sub> modified one with the same number of layers (see Figure 5 and Figure 6). These results could be explained by three effects. First of all, the integration of gold nanoparticles with comparatively large particle size constructs the multilayer films of matrix structure and extends the transfer route of glucose. As a result, more glucose in the solution could infiltrate into the multilayer films and be catalyzed by enzyme. In addition, since the difference in rigidity and charge density between colloid particles and PDDA layer could result in less dense packing [59], the permeability of multilayer films gets better improved and glucose could smoothly infiltrate through the multilayer films and effectively contact with the inside layers of enzyme. Secondly, the high surface to volume

ratio of gold nanoparticles makes more PDDA adsorbed on the gold nanoparticles and directly amplifies the surface coverage of the GOx layers. At last, though GOx is directly adsorbed on polyions membrane, gold nanoparticles still provide many binding sites through linear polyions and combined with GOx. Since the interaction between enzyme and gold nanoparticles is very strong [60] and gold nanoparticles provide an environment similar to the native environment of redox proteins [22,23], the amount and activity of GOx in the (PDDA/Au<sub>NP</sub>/PDDA/GOX)<sub>n</sub> multilayer films were both higher than those in the (PDDA/GOX)<sub>n</sub> multilayer films.

#### 4.5 Optimal Number of Multilayers for glucose response.

Figure 5 shows the linear range for glucose detection corresponding to the number of PDDA/Au<sub>NP</sub>/PDDA/GOX layers and PDDA/GOX layers modified electrodes. The linear range increases significantly as the number of multilayer films increases from one to four. An addition coating of the fifth and sixth multilayer films induces decrease of the linear range. Figure 6 shows the effect of the number (1-6) of multilayer films on the sensitivity of the biosensors. The sensitivity of the biosensors with or without gold nanoparticles increases with the number increasing from one to four multilayer films, then decreases. Thus the electrode modified with four-multilayer film, exhibited the largest linear range and highest sensitivity to glucose.

With the number of multilayer films increases, the response time increases correspondingly. Figure 7 shows the response time of the electrode modified with



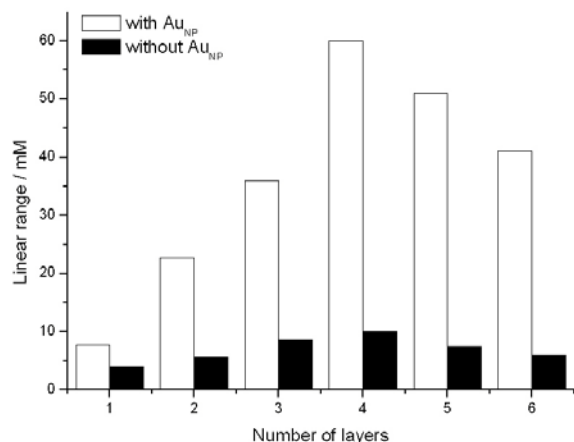


**Figure. 5** The upper limit of linear range for glucose of the  $(\text{PDDA}/\text{Au}_{\text{NP}}/\text{PDDA}/\text{GOD})_n$  modified biosensor and the  $(\text{PDDA}/\text{GOD})_n$  modified biosensor corresponding to the number of layers in 0.1 M phosphate buffer (pH 7.4).

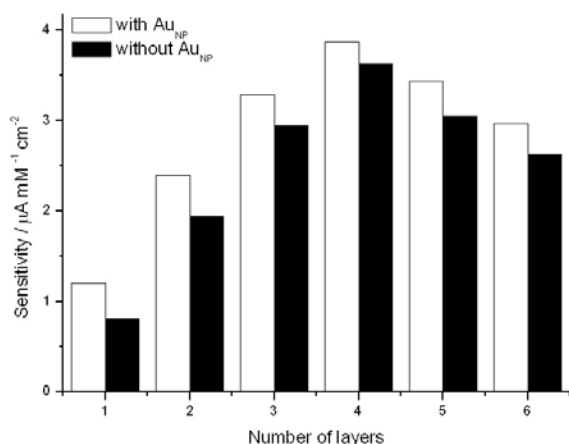


**Figure. 6.** The sensitivity of the  $(\text{PDDA}/\text{Au}_{\text{NP}}/\text{PDDA}/\text{GOD})_n$  modified biosensor and the  $(\text{PDDA}/\text{GOD})_n$  modified biosensor corresponding to the number of layers.

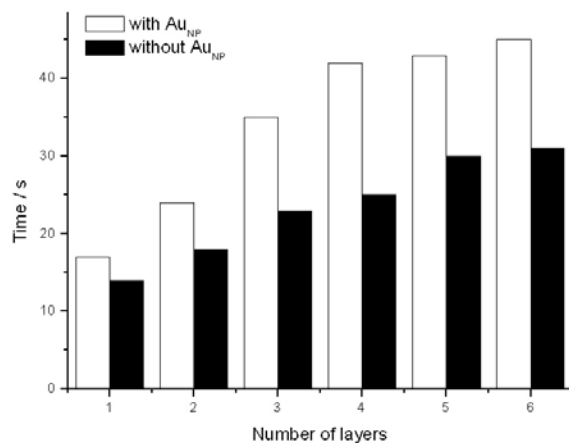


**Figure. 7.** Response time of the  $(\text{PDDA}/\text{Au}_{\text{NP}}/\text{PDDA}/\text{GOD})_n$  modified biosensor and the  $(\text{PDDA}/\text{GOD})_n$  modified biosensor corresponding to the number of layers.

layer numbers (1-6). Although  $(\text{PDDA}/\text{GOx})_n$  film is much thinner than the  $(\text{PDDA}/\text{Au}_{\text{NP}}/\text{PDDA}/\text{GOx})_n$  film with the same number of layers, the response time of  $(\text{PDDA}/\text{Au}_{\text{NP}}/\text{PDDA}/\text{GOx})_n$  film modified electrode is somewhat more than that of  $(\text{PDDA}/\text{GOx})_n$  modified electrodes due to the large permeability of the  $(\text{PDDA}/\text{Au}_{\text{NP}}/\text{PDDA}/\text{GOx})_n$  film.

#### 4.6 Effect of the Solution pH on the Biosensor Response

The effect of the pH value of the detection solution on the response behavior of the  $(\text{PDDA}/\text{Au}_{\text{NP}}/\text{PDDA}/\text{GOx})_4$  modified biosensor was studied between 6.0 and 9.0 and the corresponding result is shown in Figure 8. From Figure 8, the maximum response current can be observed at pH 8.0. The optimal pH value is somewhat large than that previous reports [61], where the GOx based biosensors usually have optimal pH values at about neutral. Generally, the effect of the solution pH on the biosensor response resulted from two factors. On one hand, since the detection of glucose is based on the oxidation of the produced hydrogen peroxide and there are protons produced, basic condition facilitates the proceeding of the reaction. Therefore, the response of the proposed biosensor will increase with the increase of pH. On the other hand, the activity of enzyme depends greatly on the pH of surrounding solution, and extreme pH conditions will result in the loss of enzyme activity. Here, the immobilized GOx can remain active at somewhat basic conditions (up to pH 8.0), indicating that the deposited gold nanoparticles provides a biocompatible microenvironment for GOx to withstand outside conditions.

#### 4.7 The Reproducibility and Stability of Biosensor

The reproducibility and storage stability of the biosensor have also been studied. The relative standard deviation (R.S.D) of the biosensor response to 2.0 mM glucose was 3.7% for 11 successive measurements. The biosensor was stored dry at 4 °C and measured at intervals of a week, and it remained about 78% of its original sensitivity after 2 months.

## 5. CONCLUSION

A novel structure of multilayer films in layer-by-layer self-assembly glucose biosensor was proposed. The introduction of gold nanoparticles proved to be effective for the construction of sensitive, stable, and extended- ranged biosensors. Thus, this strategy could be readily extended toward the preparation of other amperometric biosensors. It should be pointed out that ascorbic, uric acid and acetaminophen etc. which are oxidized electrochemically at +0.7V would interfere the determination of glucose. To resolve this problem, poly(allylamine) hydrochloride (PAA) and poly(potassium vinyl sulfate) (PVS) could be used to replace PDDA and PSS to construct a precursor film, which can effectively impede the penetration of interferences [62]. To further improve the selectivity of this kind of biosensor, we are working on the

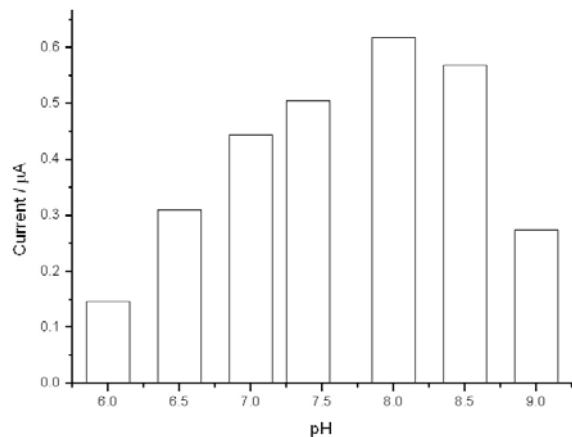


**Figure. 8** Effect of pH on the response of the (PDDA/Au<sub>NP</sub>/PDDA/GOD)<sub>4</sub> modified biosensor to 5.0 mM glucose in 0.1 M phosphate buffer.

construction of the multilayered configuration by co-integrating an electron mediator.

## 6. ACKNOWLEDGMENT

We gratefully thank the National Natural Science Foundation of China for financial support of this research (No. 20205007, 90206037).

## 7. REFERENCES

- McNichols R. J. & G. L. Cote: Optical glucose sensing in biological fluids: an overview *J Biomed Opt* 5, 5-16 (2000)
- Steffes P. G: Laser-based measurement of glucose in the ocular aqueous humor: an efficacious portal for determination of serum glucose levels. *Diabetes Technol Ther* 1, 129-133 (1999)
- Forzani E. S, V. Solis & E. J. Calvo: Electrochemical behavior of polyphenol oxidase immobilized in self-assembled structures layer by layer with cationic polyallylamine. *Anal Chem* 72, 5300-5307 (2000)
- Kros A, M. Gerritsen, V. S. I. Sprakel, N. A. J. M. Sommerdijk, J. A. Jansen & R. J. M. Nolte: Silica-based hybrid materials as biocompatible coatings for glucose sensors. *Sens Actuators B* 81, 68-75 (2001)
- Galeska I, D. Chattopadhyay & F. Moussy: Calcification-resistant Nafion/Fe<sup>3+</sup> assemblies for implantable biosensors. *Biomacromolecules* 1, 202-207 (2000)
- Kulys J: The carbon paste electrode encrusted with a microreactor as glucose biosensor. *Biosensor and Bioelectronics* 14, 473-479 (1999)
- Cowell D. C, A. A. Dowman & T. Ashcroft: The detection and identification of metal and organic pollutants in potable water using enzyme assays suitable for sensor development. *Biosensor and Bioelectronics* 10, 509-516 (1995)
- Serban S, A. F. Danet & N. J. El Murr: Rapid and sensitive automated method for glucose monitoring in wine processing. *Agric Food Chem* 52, 5588-5592 (2004)

- Chen X. H, N. Matsumoto, Y.B. Hu & G. S. Wilson: Electrochemically mediated electrodeposition/electropolymerization to yield a glucose microbiosensor with improved characteristics. *Anal Chem* 74, 368-372 (2002)
- Karyakin A. A, E. A. Kotelnikova, L. V. Lukachova & E. E. Karyakina: Optimal environment for glucose oxidase in perfluorosulfonated ionomer membranes: Improvement of first-generation biosensors. *Anal Chem* 74, 1597-1603 (2002)
- Chen W. B, H. Pardue & S. Williams: Evaluation of alternative measurement and data-processing options for enzyme-based biosensors. *Anal Chim Acta* 388, 231-242 (1999)
- Isaksen A & J. Adler-Nissen: Antioxidative effect of glucose oxidase and catalase in mayonnaises of different oxidative susceptibility .2. Mathematical modelling. *Lebensmittel-Wissenschaft und-Technologie* 30, 847-852 (1997).
- Poyard S, N. Jaffrezic-Renault, C. Martelet, S. Cosnier & P. Labbe: Optimization of an inorganic/bio-organic matrix for the development of new glucose biosensor membranes. *Anal Chim Acta* 364, 165-172 (1998)
- Reddy S. M & P. Vadama: Entrapment of glucose oxidase in non-porous poly(vinyl chloride). *Anal Chim Acta* 461, 57-64 (2002)
- Maines A, D. Ashworth & P. Vadgama: Diffusion restricting outer membranes for greatly extended linearity measurements with glucose oxidase enzyme electrodes. *Anal Chim Acta* 333, 223-231 (1996)
- Foulds N. C & C. R. Lowe: Immobilization of glucose oxidase in ferrocene-modified pyrrole polymers. *Anal Chem* 60, 2473-2478 (1988)
- Heller A: Electrical wiring of redox enzymes. *Acc Chem Res* 23, 128-134 (1990)
- Lawrence N. S, R. P. Deo & J. Wang: Biocatalytic carbon paste sensors based on a mediator pasting liquid. *Anal Chem* 76, 3735-3739 (2004)
- Cass A. E. G, G. Davis, G. D. Francis, H. A. O. Hill, W. J. Aston, I. J. Higgins, E. V. Plotkin, L. D. L. Scott & A. P. F. Turner: Ferrocene-mediated enzyme electrode for amperometric determination of glucose. *Anal Chem* 56, 667-671 (1984)
- Forrow N. J, N. C. Foulds, J. E. Frew & J. T. Law: Synthesis, characterization, and evaluation of ferrocene-theophylline conjugates for use in electrochemical enzyme immunoassay. *Bioconjugate Chem* 15, 137-144 (2004)
- Yamazaki T, K. Kojima & K. Sode: Extended-range glucose sensor employing engineered glucose dehydrogenases. *Anal Chem* 72, 4689-4693 (2000)
- Xiao Y, H. X. Ju & H. Y. Chen: Hydrogen peroxide sensor based on horseradish peroxidase-labeled Au colloids immobilized on gold electrode surface by cysteamine monolayer. *Anal Chim Acta* 391, 73-82 (1999)
- Jia J, B. Wang, A. Wu, G. Cheng, Z. Dong & S. Li: A method to construct a third-generation horseradish peroxidase biosensor: self-assembling gold nanoparticles to three-dimensional sol-gel network. *Anal Chem* 74, 2217-2223 (2002)
- Luo X. L, J. J. Xu, Y. Du & H. Y. Chen: A glucose biosensor based on electrodeposited chitosan-glucose



- oxidase-gold nanoparticles biocomposite. *Analytical Biochemistry* in press
25. Decher G & J.-D. Hong: Buildup of ultrathin multilayer films by a self-assembly process. I. Consecutive adsorption of anionic and cationic bipolar amphiphiles on charged surfaces. *Macromol Chem Macromol Symp* 46, 321-327 (1991)
26. Lvov Y, K. Anga, I. Ichinose & T. Kunitake: Assembly of multicomponent protein films by means of electrostatic layer-by-layer adsorption. *J Am Chem Soc* 117, 6117-6123 (1995)
27. Mizutani F, Y. Sato, S. Yabuki & Y. Hirata: Enzyme ultra-thin-layer electrode prepared by the co-adsorption of poly-L-lysine and glucose oxidase onto a mercaptopropionic acid-modified gold surface. *Chem Lett* 4, 251-252 (1996)
28. Hou S. F, H. Q. Fang & H. Y. Chen: An amperometric enzyme electrode for glucose using immobilized glucose oxidase in a ferrocene attached poly(4-vinylpyridine) multilayer film. *Anal Lett* 30, 1631-1641 (1997)
29. Hodak J, R. Etchenique, E. J. Calvo, K. Singhal & P. N. Bartlett: Layer-by-layer self-assembly of glucose oxidase with a poly(allylamine)ferrocene redox mediator. *Langmuir* 13, 2708-2716 (1997)
30. Hou S. F, K. S. Yang, H. Q. Fang & H. Y. Chen: Amperometric glucose enzyme electrode by immobilizing glucose oxidase in multilayers on self-assembled monolayers surface. *Talanta* 47, 561-567 (1998)
31. Sirkar K, A. Revzin & M. V. Pishko: Glucose and lactate biosensors based on redox polymer/oxidoreductase nanocomposite thin films. *Anal Chem* 72, 2930-2936 (2000)
32. Calvo E.J, R. Etchenique, L. Pietrasanta, A. Wolosiuk & C. Danilowicz: Layer-by-layer self-assembly of glucose oxidase and Os(Bpy)<sub>2</sub>ClPyCH<sub>2</sub>NH-poly(Allylamine) Bioelectrode. *Anal Chem* 73, 1161-1168 (2001)
33. Sun Y.P, J. Q. Sun, X. Zhang, C. Q. Sun, Y. Wang & J. C. Shen: Chemically modified electrode via layer-by-layer deposition of glucose oxidase (GOD) and polycation-bearing Os complex. *Thin Solid Films* 327, 730-733 (1998)
34. Forzani E. S, M. Otero, M. A. Perez, M. L. Teijelo & E. J. Calvo: The structure of layer-by-layer self-assembled glucose oxidase and Os(Bpy)<sub>2</sub>ClPyCH<sub>2</sub>NH-Poly(allylamine) multilayers: ellipsometric and quartz crystal microbalance studies. *Langmuir* 18, 4020-4029 (2002)
35. Calvo E. J, C. Danilowicz & A. Wolosiuk: Molecular "wiring" enzymes in organized nanostructures. *J Am Chem Soc* 124, 2452-2453 (2002)
36. Yoon H. C, M. Y. Hong & H. S. Kim: Functionalization of a poly(amidoamine) dendrimer with ferrocenyls and its application to the construction of a reagentless enzyme electrode. *Anal Chem* 72, 4420-4427 (2000)
37. Berchmans S, R. Sathyajith & V. Yegnaman: Layer-by-layer assembly of 1,4-diaminoanthraquinone and glucose oxidase. *Mater Chem Phys* 77, 390-396 (2003)
38. Anzai J, H. Takeshita, Y. Kobayashi, T. Osa & T. Hoshi: Layer-by-layer construction of enzyme multilayers on an electrode for the preparation of glucose and lactate sensors: Elimination of ascorbate interference by means of an ascorbate oxidase multilayer. *Anal Chem* 70, 811-817 (1998)
39. Kobayashi Y & J. Anzai: Preparation and optimization of bienzyme multilayer films using lectin and glyco-enzymes for biosensor applications. *Journal of Electroanalytical Chemistry* 507, 250-255 (2001)
40. Anzai J. I, Y. Kobayashi, Y. Suzuki, H. Takeshita, Q. Chen, T. Osa, T. Hoshi & X. Y. Du: Enzyme sensors prepared by layer-by-layer deposition of enzymes on a platinum electrode through avidin-biotin interaction. *Sensors and Actuators B* 52, 3-9 (1998)
41. Trau D & R. Renneberg: Encapsulation of glucose oxidase microparticles within a nanoscale layer-by-layer film: immobilization and biosensor applications. *Biosensors and Bioelectronics* 18, 1491-1499 (2003)
42. Ferreira M, P. A. Fiorito, N. Osvaldo, J. Oliveira & S. I. Cordoba de Torresi: Enzyme-mediated amperometric biosensors prepared with the Layer-by-Layer (LbL) adsorption technique. *Biosensors and Bioelectronics* 19, 1611-1615 (2004)
43. Hao E & T. Lian: Buildup of polymer/Au nanoparticle multilayer thin films based on hydrogen bonding. *Chem Mater* 12, 3392-3396 (2000)
44. Ostrander J. W, A. A. Mamedov & N. A. Kotov: Two modes of linear layer-by-layer growth of nanoparticle-polyelectrolyte multilayers and different interactions in the layer-by-layer deposition. *J Am Chem Soc* 123, 1101-1110 (2001)
45. Kotov N. A, I. Dekany & J. H. Fendler: Layer-by-layer self-assembly of polyelectrolyte-semiconductor nanoparticle composite films. *J Phys Chem* 99, 13065-13069 (1995)
46. Hua F, T. H. Cui & Y. M. Lvov: Ultrathin cantilevers based on polymer-ceramic nanocomposite assembled through layer-by-layer adsorption. *Nano Lett* 4, 823-825 (2004)
47. Musick M. D, C. D. Keating, M. H. Keefe & M. J. Natan: Stepwise construction of conductive Au colloid multilayers from solution. *Chem Mater* 9, 1499-1501 (1997)
48. Zhang X, F. Shi, X. Yu, H. Liu, Y. Fu, Z. Q. Wang, L. Jiang & X. Y. Li: Polyelectrolyte multilayer as matrix for electrochemical deposition of gold clusters: toward superhydrophobic surface. *J Am Chem Soc* 126, 3064-3065 (2004)
49. Henglein A: Small-particle research: Physicochemical properties of extremely small colloidal metal and semiconductor particles. *Chem Rev* 89, 1861-1873 (1989)
50. Shipway A. N, M. Lahav & I. Willner: Nanostructured gold colloid electrodes. *Adv Mater* 12, 993-998 (2000)
51. Yu A. M, Z. J. Liang, J. H. Cho & F. Caruso: Nanostructured electrochemical sensor based on dense gold nanoparticle films. *Nano Lett* 3, 1203-1207 (2003)
52. Musick M. D, C. D. Keating, A. Lyon, S. L. Botsko, D. J. Pena, W. D. Holliday, T. M. McEvoy, J. N. Richardson, & M. J. Natan: Metal films prepared by stepwise assembly. 2. Construction and characterization of colloidal Au and Ag multilayers. *Chem Mater* 12, 2869-2881 (2000)
53. Brust M. D, Bethell, C. J. Kiely & D. J. Schiffrin: Self-assembled gold nanoparticle thin films with nonmetallic optical and electronic properties. *Langmuir* 14, 5425-5429 (1998)
54. Joseph V. I. Besnard, M. Rosenberger, B. Guse, H. Nothofer, J. M. Wessels, U. Wild, A. Knop-Gericke, D. S.

Su, R. Schlogel, A. Yasuda & T. Vossmeier: Self-assembled gold nanoparticle/alkanedithiol films: preparation, electron microscopy, XPS-analysis, charge transport, and vapor-sensing properties. *J Phys Chem B* 107, 7406-7413 (2003)

55. Xiao Y, H. X. Ju & H. Y. Chen: Hydrogen peroxide sensor based on horseradish peroxidase-labeled Au colloids immobilized on gold electrode surface by cysteamine monolayer. *Anal Chim Acta* 391, 73-82 (1999)

56. Neiman B, E. Grushka & O. Lev: Use of gold nanoparticles to enhance capillary electrophoresis. *Anal Chem* 73, 5220-5227 (2001)

57. Guo Z. H, Y. Shen, M. K. Wang, F. Zhao & S. J. Dong: Electrochemistry and Electrogenerated Chemiluminescence of SiO<sub>2</sub> Nanoparticles/Tris(2,2'-bipyridyl)ruthenium(II) Multilayer Films on Indium Tin Oxide Electrodes. *Anal Chem* 76, 184-191 (2004)

58. Ram M. K, M. Salerno, M. Adami, P. Faraci & C. Nicolini: Physical properties of polyaniline films: Assembled by the layer-by-layer technique. *Langmuir* 15, 1252-1259 (1999)

59. Lvov Y, K. Ariga, M. Onda, I. Ichinose & T. Kunitake: Alternate assembly of ordered multilayers of SiO<sub>2</sub> and other nanoparticles and polyions. *Langmuir* 13, 6195-6203 (1997)

60. Gole A, C. Dash, V. Ramakrishnan, S. R. Sainkar, A. B. Mandale, M. Rao & M. Sastry: Pepsin-gold colloid conjugates: preparation, characterization, and enzymatic activity. *Langmuir* 17, 1674-1679 (2001)

61. Zhang D, K. Zhang, Y. L. Yao, X. H. Xia & H.Y. Chen: Multilayer assembly of prussian blue nanoclusters and enzyme-immobilized poly(toluidine blue) films and its application in glucose biosensor construction. *Langmuir* 20, 7303-7307 (2004)

62. Hoshi T, H. Saiki, S. Kuwazawa, C. Tsuchiya, Q. Chen & J. Anzai: Selective permeation of hydrogen peroxide through polyelectrolyte multilayer films and its use for amperometric biosensors. *Anal Chem* 73, 5310-5315 (2001)

**Abbreviations:** PE: polyelectrolyte; PDDA: poly(dimethyldiallylammonium chloride); PSS: poly(sodium 4-styrenesulfonate); PAA: poly(allylamine) hydrochloride; PVS: poly(potassium vinyl sulfate); GOx: glucose oxidase; Lox: lactate oxidase; AOx: ascorbate oxidase; HRP: horseradish peroxidase; Au<sub>NP</sub>: gold nanoparticle; MPS: 3-mercapto-1-propanesulfonic acid, sodium salt; Fc-D: ferrocenyl-tethered dendrimers; DAAQ: 1,4-diaminoanthraquinone; LBL: layer-by-layer assembly; EIS: Electrochemical impedance spectroscopy; UV-Vis: Ultraviolet and visible; TEM: transmission electron microscopy.

**Key Words:** Gold nanoparticles (Au<sub>NP</sub>); glucose oxidase (GOD); Polyelectrolyte multilayer (PEM); Layer-by-layer self-assembly; Glucose biosensor

**Send correspondence to:** Dr Jing-Juan Xu, Key Lab of Analytical Chemistry for Life Science, Department of Chemistry, Nanjing University, Nanjing 210093, P.R. China, Tel: +86-25-83597294, Fax: +86-25-83594862, E-mail: xujj@nju.edu.cn

<http://www.bioscience.org/current/vol10.htm>